This work has resulted in new thermodynamic tables that have an expanded range based on sound experimental data.

### Acknowledgment

The authors wish to thank Mr. E. A. E. Lund and Mr. J. B. Moore for their assistance in collecting the physical properties. Thanks are also due to Dr. E. Rosenthal for applying computer programs, developed for earlier work, in computation of constants for the various equations, correlating the data, and producing the thermodynamic tables.

### Glossary

| | |
|---|---|
| $A$-F | constants in vapor pressure equation |
| $A_d$, $B_d$, $C_a$, $D_d$ | constants in liquid density equation |
| $A_i$, $B_i$, $C_i$, $b$ | constants in $P-V-T$ equation |
| $A_c$-$E_c$ | constants in heat capacity equation |
| $C_P$ | ideal heat capacity of gas btu/(lb/mol °R) |
| $D_{cr}$ | critical density lb/ft$^3$ |
| $H$ | enthalpy, btu/lb |
| $K$ | constant in $P-V-T$ equation |
| $P$ | absolute pressure lb/in.$^2$ |
| $R$ | gas constant |
| $S$ | entropy |
| $T$ | absolute temperature, °R |
| $T_c$ | critical temperature, °R |
| $V$ | volume, ft$^3$/lb |

### Literature Cited

(1) Benning, A. F., McHarness, R. C., *Ind. Eng. Chem.*, **32**, 497-499 (1940).
(2) Benning, A. F., McHarness, R. C., *Ind. Eng. Chem.*, **32**, 698 (1940).
(3) Benning, A. F., McHarness, R. C., *Ind. Eng. Chem.*, **32**, 814 (1940).
(4) Cailletet, Mathias, *J. Phys.*, **5**, 549 (1886).
(5) Douslin, D. R., Morre, R. T., Dawson, J. P., Waddington, G., *J. Am. Chem. Soc.*, **80**, 2031 (1958).
(6) Ernst, G., Busser, J., *J. Chem. Thermodyn.*, **2**, 787-791 (1970).
(7) Higgins, E. R., Lielmezs, J., *J. Chem. Eng. Data*, **10**, 178-179 (1965).
(8) Hiraoka, H., Hildebrand, J. M., *J. Phys. Chem.*, **67**, 916 (1963).
(9) Hovorka, F., Geiger, F., *J. Am. Chem. Soc.*, **55**, 4759-4761 (1933).
(10) Martin, J. J., Hou, Y. C., *AIChE J.*, **5**, 125-129 (1959).
(11) Martin, J. J., Hou, Y. C., *AIChE J.*, **1**, 142 (1959).
(12) Martin, J. J., Kapoor, R. M., DeNevers, N., *AIChE J.*, **5**, 1959 (1959).
(13) Martin, J. J., *Am. Soc. Mech. Eng.* [*Pap.*], 110 (1959).
(14) Ridel, L., *Z. Gesamte Kaelte-Ind.*, **45**, 221-225 (1938).
(15) Sinka, J. V., Murphy, K. P., *J. Chem. Eng. Data*, **12**, 315 (1967).
(16) Speciality Chemicals Division, Allied Chemical Corp.
(17) White, D., Hilsenrath, J., *Rev. Sci. Instrum.*, **29**, 648 (1958).

Received for review November 23, 1976. Accepted January 30, 1978.

# Vapor Pressure of Aluminum Chloride Systems. 2. Pressure of Unsaturated Aluminum Chloride Gas

**John T. Viola, Armand A. Fannin, Jr., Lowell A. King,* and David W. Seegmiller**

*Frank J. Seiler Research Laboratory (Air Force Systems Command) and Department of Chemistry and Biological Sciences, United States Air Force Academy, Colorado 80840*

**The pressures and volumes of unsaturated, gaseous samples of aluminum chloride were measured from 167 to 277 °C. The samples were contained in a variable-volume Pyrex isoteniscope which utilized mercury as the manometric fluid. The mercury columns were brought to null by an external pressure which was in turn measured at each experimental point. The experimental values of temperature, pressure, and volume were fit to a van der Waals equation of state, giving $a = 4.285 \times 10^{10}$ cm$^6$ Torr mol$^{-2}$ and $b = 178.9$ cm$^3$ mol$^{-1}$.**

As part of an investigation of certain low-melting, molten salt electrolytes for high-energy density batteries, we needed to know the vapor density and vapor pressure of aluminum chloride. We have made these measurements for aluminum chloride vapor in equilibrium with the liquid or solid (*4*, *6*, *8*). Only a few measurements have been made on unsaturated gaseous aluminum chloride (*2*, *7*, *9*); these were concerned with determining the dissociation constant for the reaction $Al_2Cl_6(g) \rightleftarrows 2AlCl_3(g)$ and were made at higher temperatures than were of interest in the present work.

### Experimental Section

Crystals of aluminum chloride were loaded into the Pyrex isoteniscope shown in Figure 1. Preparation of the aluminum chloride, loading of the isoteniscope, and the constant temperature bath and its temperature regulation and measurement were all as described previously (*8*). Sample pressures were also determined as before (*8*), but the external pressures were read by the capacitance manometer only in the present work.

Five samples of $Al_2Cl_6$ were used. The masses of samples I through V were 0.2512, 0.5790, 0.5978, 0.7499, and 1.0430 g, respectively. Estimated uncertainty in mass was ±0.0002 g. It was necessary to know not only the gas volume above each index mark on the bulb but also the total amount of mercury below each index mark, including the mercury in the two side arms. Additionally, the volume changes per unit length for the center compartment in the vicinity of each index mark and for the left-hand side arm were required. These volume calibrations were made by recording heights and weighing the apparatus when it contained varying amounts of water or mercury. These calibration data are given in Table I.

Measurements were made according to the following procedure. The evacuated isoteniscope (without mercury) and sample crystal were manipulated so that the crystal rested on the sample shelf. The isoteniscope was then immersed in a room temperature bath and connected to the pressure measurement device. Enough mercury was introduced to block the entrance to the middle compartment, and the bath was warmed to the desired beginning temperature. It was necessary to add mercury from time to time as the $Al_2Cl_6$ pressure increased. At the measurement temperature, internal pressure was sufficient to maintain a continuous column of mercury from the inner bulb to the stopcock at the mercury reservoir. The initial measurement was made on each sample by carefully admitting just enough mercury to cause the mercury columns to be at the

Table I. Calibration Data[a]

| Index mark | Gas volume above mark, cm³ | Total Hg volume below mark, cm³ | Linear volume change, cm³/cm | |
|---|---|---|---|---|
| | | | Center compt | Side arm |
| a | 177.1 ± 0.2 | 11.48 | 1.48[b] | |
| b | 133.7 ± 0.4 | 55.42 | | |
| c | 85.5 ± 0.3 | 104.55 | 12.85 ± 0.08 | 0.20 ± 0.01 |
| d | 37.5 ± 0.4 | 153.28 | | |

[a] All calibration data have been corrected for thermal expansion of glass, water, and mercury and for air buoyancy in weighing. [b] During pressure measurements, the meniscus remained near enough to index mark a that the error introduced by assuming a cylindrical cross section rather than the real conical cross section could be neglected.

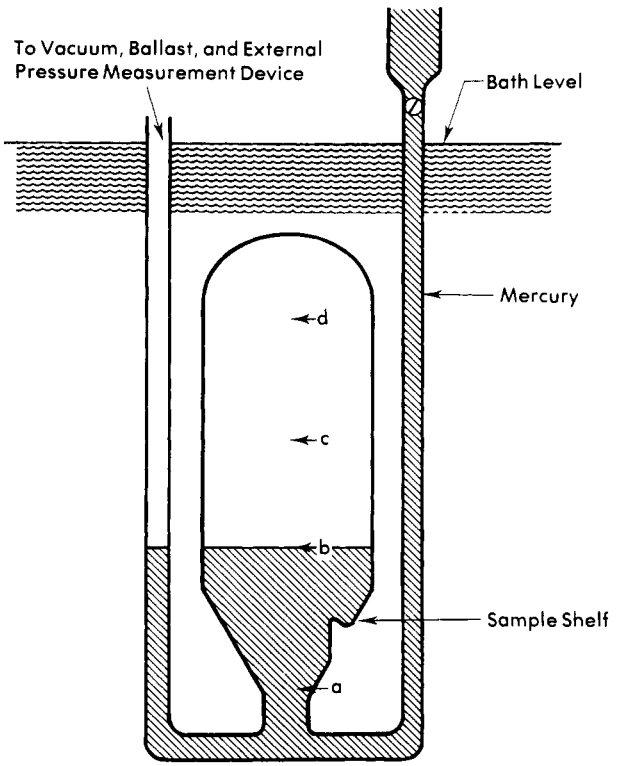


**Figure 1.** Isoteniscope.

same level when the inner meniscus was at index mark a.

Without changing the amount of mercury in the isoteniscope, the bath temperature was raised and lowered to values about the initial temperature, and the pressure was measured at each temperature. As the glassware and mercury expanded or contracted with temperature, the inner compartment meniscus in general would not be at the index mark when the two menisci were at the same height. By knowing the appropriate coefficients of expansion and the calibration data given in Table I, one could calculate the actual gas-phase volume at each temperature. We used $3 \times 10^{-5}$ K$^{-1}$ for the coefficient of linear expansion of Pyrex and Sears' equation (*5*) for the specific volume of mercury.

When the temperature and pressure region accessible with the meniscus near index mark a was covered, additional mercury was added from the reservoir to place the menisci at the same height as index mark b. The temperature was again varied and pressures were measured as described above. The same procedure was followed at index marks c and d. It was possible to move the meniscus from mark d back to mark c, and this was done with some of the samples. Because of the height of the mercury in the reservoir above the isoteniscope, it was not convenient to move the meniscus back to marks b or a.

For various reasons, the two menisci were not at the same level for 15 pressure measurements. In these cases the inner compartment meniscus was placed at an index mark, and the difference in meniscus heights was measured with the aid of a cathetometer, and appropriate pressure and volume corrections were calculated. There were ten measurements at index mark a for which the gas pressure was insufficient to maintain the right-hand mercury column at the reservoir stopcock. Again, appropriate volume corrections were calculated for these data points. (The volume change per unit length for the right-hand side arm was the same as for the left-hand arm, given in Table I.)

A total of 313 measurements were taken over the range 167–277 °C, 149–2950 Torr, and 9440–188 000 cm³ (molar volume). The data are given in Table II. Pressures have been corrected for the vapor pressure of mercury within the isoteniscope. Interaction between $Al_2Cl_6$ and gaseous Hg was assumed to be negligible.

## Results and Discussion

We assumed the behavior of gaseous $Al_2Cl_6$ in the region of our experimental measurements could be represented adequately by the van der Waals equation of state.

$$(P + (a/\bar{V}^2))(\bar{V} - b) = RT \qquad (1)$$

The data given in Table II approach the liquid–gas equilibrium vapor pressure line; therefore, we chose to include the saturated data of the previous paper in this series (*8*) in the data set to be fit to eq 1. In fact, some of the supposedly unsaturated gas data points actually were saturated; generally, it was not possible to detect visually a very small amount of liquid $Al_2Cl_6$ condensed on the wall of the isoteniscope. The calculated molar volume for each data point in the present work was compared with the saturated molar volume at that temperature. The latter volume was calculated from equations for the saturated vapor pressure (*8*) and orthobaric vapor density (*4*). If the supposedly unsaturated molar volume was smaller than the saturated molar volume, condensation must have taken place, and the point was eliminated from the set to be fit to eq 1. The 33 data sets rejected in this manner do not appear in Table II.

All but four of the 80 liquid–gas-saturated vapor data reported earlier (*8*) were included in the data set fit to eq 1. Molar volumes were calculated for these points as described above. The four eliminated points were at temperatures below 188.8 °C, the minimum temperature for which the orthobaric vapor density was available (*4*). The saturated data fall in the range 190–256 °C, 1616–5512 Torr, and 4640–17 100 cm³ (molar volume).

We chose to least-squares fit the data in such a way as to minimize the perpendicular distance from the experimental point to the function surface in $p$, $\bar{V}$, and $T$ given by eq 1. This procedure is a three-dimensional analogue of the fitting procedure used earlier (*8*) and depicted in Figure 2 of that report. As in that instance, the perpendicular $z$ does not quite contact the curve for eq 1 but contacts a plane drawn through the projections parallel to the $p$, $\bar{V}$, and $T$ axes of the experimental point onto the curve. The root mean square value of the quantity $|(z - \text{true perpendicular})|/(\text{true perpendicular})$ was 0.003.

We solved for values of $a$ and $b$ which minimized the sum $\sum_{i=1}^{N}(z_i)^2$ where

$$z_i = \left[ \frac{1}{\left(\frac{\delta p_i}{\Delta p_i}\right)^2 + \left(\frac{\delta \bar{V}_i}{\Delta \bar{V}_i}\right)^2 + \left(\frac{\delta T}{\Delta T_i}\right)^2} \right]^{1/2} \quad (2)$$

Equation 2 was derived elsewhere (*1*). In eq 2, $\delta T$ was assumed to be 1.0 K, and the remaining two uncertainties varied from point to point as

$$\delta p_i = 0.005 p_i$$

and, since $\bar{V}_i = V_i M / m_i$

$$\delta \bar{V}_i(\mathrm{cm}^3) = \left(\frac{\partial \bar{V}_i}{\partial V_i}\right)\delta V + \left(\frac{\partial \bar{V}_i}{\partial m_i}\right)\delta m = \frac{M}{m_i}(0.5) + \frac{V_i M}{m_i^2}(0.0002)$$

The remaining terms in eq 2 are defined as

$$\Delta p_i = p_i - \left(\frac{RT_i}{\bar{V}_i - b} - \frac{a}{\bar{V}_i^2}\right)$$

$$\Delta T_i = T_i - [(p_i + (a/\bar{V}_i^2))(\bar{V}_i - b)]/R$$

$$\Delta \bar{V}_i = \bar{V}_i - \left[\frac{RT_i}{p_i + (a/\bar{V}_j^2)} + b\right]_{\text{iterated}}$$

where iterations were performed with $\bar{V}_j$ set initially at $RT_i/P_i$ and continued until the change in $\bar{V}_j \leq 0.001$ cm$^3$.

The least-squares fit was iterative. Iterations were continued until

$$\frac{2|(\sigma - \sigma_{\text{previous iteration}})|}{\sigma + \sigma_{\text{previous iteration}}} < 10^{-8}$$

where $\sigma$, the standard deviation, was calculated from

$$\sigma = \left[\frac{1}{N-2}\sum_{i=1}^{N} z_i^2\right]^{1/2} \quad (3)$$

The values of $a$ and $b$ when the criterion of eq 3 was first satisfied were $a = 4.285 \times 10^{10}$ cm$^6$ Torr mol$^{-2}$ and $b = 178.9$ cm$^3$ mol$^{-1}$. For the entire data set the root mean square errors in pressure, volume, and temperature were 0.9, 1.6, and 0.1%, respectively.

The van der Waals constants may also be calculated from the critical density, 0.5073 g cm$^{-2}$, and critical temperature, 355.2 °C, of $Al_2Cl_6$ (*6*). The calculation yields $a = 2.31 \times 10^{10}$ cm$^6$ Torr mol$^{-2}$ and $b = 175$ cm$^3$. Since in general $a$ and $b$ are known to vary with pressure and temperature, the agreement appears reasonable, considering the temperature difference between the critical point and the range of experimental measurements. In fact, the very close agreement in $b$ is probably fortuitous.

The unsaturated data are shown in Figure 2. For clarity, the liquid–gas saturation line is shown instead of the saturated data points. The latter would be virtually indistinguishable from the line at the scale of the figure. Isotherms and isochores were calculated from eq 1, using the least-squares fit values of $a$ and $b$.

Aluminum chloride in the vapor phase exists largely as the dimer $Al_2Cl_6$ in the temperature range of the present work (*2*, *7*, *9*). From the JANAF Tables (*3*) one may calculate the dimer dissociation constant. For only three data points (on the right-rear of the surface depicted in Figure 2) was as much as 0.5% of the dimer dissociated. For all other points, the error introduced by neglecting dissociation was insignificant.

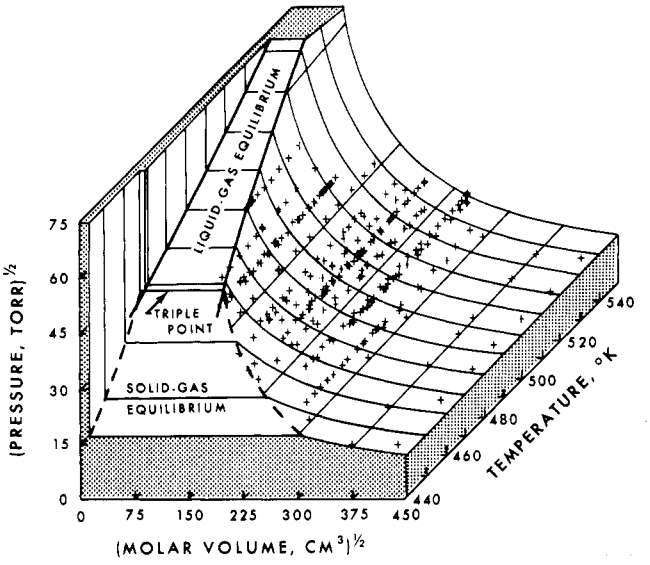


**Figure 2.** Phase diagram of $Al_2Cl_6$. Pressure and volume scales are compressed for clarity.

## Safety

Appropriate precautions should be taken for the containment of high-pressure gases in glass vessels. It was also important to consider that mercury has an appreciable vapor pressure at elevated temperatures (ca. 145 Torr at the highest temperature reached in the present study).

## Glossary

| | |
|---|---|
| $a$ | fitted constant in van der Waals equation |
| $b$ | fitted constant in van der Waals equation |
| $i$ | index for individual points |
| $j$ | index |
| $m$ | mass of $Al_2Cl_6$ in isoteniscope, g; 1.0000 g for saturated data |
| $M$ | molecular weight of $Al_2Cl_6$: 266.67 g mol$^{-1}$ |
| $N$ | the total number of experimental points used for a least-squares fit |
| $p$ | pressure, Torr |
| $R$ | universal gas constant: 62362 cm$^3$ Torr K$^{-1}$ mol$^{-1}$ |
| $T$ | temperature, K |
| $V$ | gas-phase volume in isoteniscope, cm$^3$; for saturated data, the volume of 1.0000 g calculated from vapor-density measurements |
| $\bar{V}$ | molar volume, cm$^3$ mol$^{-1}$ |
| $z$ | perpendicular distance to plane along curve; function to be treated by least-squares fitting |
| $\delta m$ | estimated uncertainty in mass of sample, 0.0002 g |
| $\delta p$ | estimated uncertainty in pressure measurement; calculated for each point |
| $\delta T$ | estimated uncertainty in temperature of sample; 1.0 K |
| $\delta V$ | estimated uncertainty in volume of sample, 0.5 cm$^3$ |
| $\delta \bar{V}$ | estimated uncertainty in molar volume of sample; calculated for each point |
| $\Delta\xi$ | the difference between the experimentally measured value of the quantity $\xi$ and the value of $\xi$ calculated from eq 1 and the remaining variables ($\xi = p$, $\bar{V}$, or $T$) |
| $\sigma$ | standard deviation |

Table II. Experimental Data

| t, °C | p, Torr | V, cm³ | t, °C | p, Torr | V, cm³ | t, °C | p, Torr | V, cm³ | t, °C | p, Torr | V, cm³ |
|---|---|---|---|---|---|---|---|---|---|---|---|
| | Sample I | | 237.84 | 507.7 | 134.07 | 232.88 | 796.9 | 86.11 | 231.84 | 498.0 | 177.41 |
| 167.34 | 195.8 | 132.60 | 238.06 | 1694.7 | 36.41 | 235.49 | 530.9 | 133.51 | 236.67 | 2220.6 | 37.11 |
| 170.64 | 149.1 | 174.17 | 239.60 | 773.6 | 85.06 | 237.38 | 390.3 | 177.41 | 238.69 | 505.6 | 177.40 |
| 173.28 | 306.2 | 85.61 | 239.60 | 783.5 | 84.94 | 237.57 | 1702.3 | 37.61 | 239.63 | 1019.6 | 85.32 |
| 185.94 | 203.1 | 132.71 | 240.51 | 777.2 | 85.05 | 238.09 | 808.1 | 86.02 | 242.48 | 668.1 | 133.84 |
| 192.72 | 155.2 | 174.45 | 240.62 | 781.6 | 85.05 | 239.74 | 810.6 | 85.99 | 243.25 | 511.5 | 177.40 |
| 198.40 | 704.1 | 37.59 | 240.62 | 1683.8 | 36.34 | 240.51 | 1719.3 | 37.53 | 246.55 | 2232.4 | 36.84 |
| 204.18 | 325.6 | 85.06 | 241.06 | 1086.5 | 61.29 | 241.41 | 536.9 | 133.45 | 248.42 | 517.2 | 177.40 |
| 206.65 | 212.9 | 132.97 | 243.47 | 1091.2 | 61.24 | 244.71 | 1744.3 | 37.41 | 249.03 | 677.7 | 133.78 |
| 208.06 | 165.2 | 177.42 | 243.69 | 1720.6 | 36.26 | 245.12 | 409.6 | 177.41 | 249.91 | 1047.4 | 85.13 |
| 220.15 | 167.5 | 175.11 | 245.04 | 1724.7 | 36.22 | 245.51 | 1757.8 | 37.39 | 253.65 | 523.6 | 177.40 |
| 220.15 | 746.7 | 37.00 | 245.78 | 793.1 | 84.83 | 246.41 | 543.8 | 133.41 | 257.07 | 690.0 | 133.71 |
| 222.60 | 220.4 | 133.28 | 246.00 | 1710.1 | 36.19 | 246.69 | 824.4 | 85.86 | 257.82 | 526.4 | 177.40 |
| 224.30 | 340.5 | 84.69 | 247.10 | 1099.9 | 61.15 | 246.77 | 1763.6 | 37.36 | 260.72 | 1075.6 | 84.94 |
| 230.28 | 225.6 | 133.49 | 248.59 | 1738.2 | 36.12 | 248.75 | 1759.9 | 37.30 | 264.73 | 700.9 | 133.64 |
| 234.34 | 160.2 | 175.30 | 249.50 | 1730.0 | 36.10 | 249.47 | 828.9 | 85.81 | 265.67 | 1086.0 | 84.85 |
| 244.79 | 800.1 | 36.33 | 249.80 | 798.8 | 84.75 | 249.66 | 547.1 | 133.38 | 265.72 | 532.3 | 177.40 |
| 250.32 | 232.2 | 133.31 | 250.24 | 1102.4 | 61.08 | 251.45 | 1779.0 | 37.23 | 270.79 | 537.1 | 177.40 |
| 263.07 | 231.8 | 133.19 | 250.76 | 523.9 | 133.95 | 252.80 | 549.1 | 133.35 | 273.87 | 544.2 | 177.40 |
| 264.40 | 839.6 | 35.79 | 250.82 | 392.2 | 177.41 | 254.15 | 837.5 | 85.73 | 274.56 | 538.7 | 177.39 |
| 264.45 | 175.6 | 176.88 | | | | 254.98 | 840.3 | 85.71 | | | |
| 264.51 | 367.2 | 83.96 | | Sample III | | 256.19 | 840.9 | 85.69 | | Sample V | |
| | | | 179.55 | 359.7 | 177.43 | 256.72 | 417.9 | 177.41 | 180.41 | 615.1 | 177.45 |
| | Sample II | | 181.43 | 710.5 | 86.28 | 256.91 | 843.4 | 85.68 | 189.61 | 628.9 | 177.45 |
| 194.77 | 1469.9 | 37.59 | 183.72 | 362.5 | 177.43 | 257.52 | 553.6 | 133.31 | 194.88 | 1242.4 | 86.01 |
| 196.88 | 1479.6 | 37.53 | 184.45 | 719.7 | 86.22 | 258.62 | 846.1 | 85.65 | 197.21 | 640.2 | 177.45 |
| 197.15 | 467.9 | 134.42 | 186.61 | 365.3 | 177.43 | 261.49 | 557.4 | 133.27 | 201.76 | 1264.4 | 85.89 |
| 198.08 | 978.9 | 62.26 | 190.31 | 1523.7 | 37.91 | 262.46 | 853.7 | 85.58 | 202.93 | 836.3 | 133.90 |
| 200.98 | 716.6 | 85.64 | 190.53 | 367.5 | 177.43 | 264.42 | 438.6 | 177.41 | 204.72 | 651.5 | 177.45 |
| 201.17 | 987.4 | 62.19 | 192.50 | 479.6 | 133.88 | 265.25 | 559.6 | 133.24 | 208.79 | 655.8 | 177.45 |
| 204.31 | 1514.9 | 37.33 | 193.50 | 370.8 | 177.43 | 267.72 | 864.7 | 85.48 | 210.40 | 850.9 | 133.83 |
| 204.34 | 994.9 | 62.12 | 193.83 | 1543.9 | 37.82 | 269.41 | 563.9 | 133.20 | 213.96 | 663.8 | 177.45 |
| 205.97 | 477.6 | 134.34 | 196.34 | 483.8 | 133.85 | 269.88 | 869.5 | 85.44 | 214.86 | 1308.2 | 85.65 |
| 207.73 | 725.1 | 85.64 | 196.72 | 1555.9 | 37.74 | 272.34 | 566.8 | 133.18 | 215.11 | 1309.2 | 85.65 |
| 208.82 | 1532.7 | 37.21 | 197.70 | 373.8 | 177.42 | 272.34 | 875.7 | 85.40 | 215.32 | 1310.1 | 85.64 |
| 209.23 | 1004.0 | 62.01 | 200.68 | 376.1 | 177.42 | 272.90 | 874.5 | 85.39 | 216.74 | 863.1 | 133.77 |
| 209.28 | 727.8 | 85.49 | 201.76 | 491.0 | 133.80 | 273.09 | 875.6 | 85.38 | 217.09 | 2735.0 | 37.69 |
| 211.89 | 733.5 | 85.44 | 202.14 | 1585.6 | 37.59 | 274.15 | 568.6 | 133.16 | 218.57 | 2745.2 | 37.65 |
| 212.36 | 728.5 | 85.56 | 202.44 | 1589.8 | 37.59 | 276.31 | 576.5 | 133.14 | 218.62 | 2709.7 | 37.65 |
| 212.71 | 1546.6 | 37.11 | 204.18 | 1604.6 | 37.55 | 276.84 | 578.9 | 133.14 | 220.28 | 673.1 | 177.44 |
| 213.04 | 1013.8 | 61.93 | 205.37 | 495.7 | 133.77 | 277.20 | 581.4 | 133.13 | 220.37 | 2728.5 | 37.60 |
| 214.21 | 479.0 | 134.11 | 205.70 | 760.1 | 85.84 | 277.42 | 580.3 | 133.13 | 220.88 | 2735.5 | 37.59 |
| 216.17 | 479.6 | 134.09 | 205.72 | 379.8 | 177.42 | | | | 223.37 | 877.3 | 137.72 |
| 216.17 | 487.0 | 134.26 | 206.54 | 1606.5 | 38.29 | | Sample IV | | 223.42 | 2742.9 | 37.52 |
| 217.12 | 1563.2 | 36.99 | 208.55 | 381.9 | 177.42 | 184.18 | 881.0 | 86.32 | 224.13 | 1338.2 | 85.48 |
| 217.61 | 367.1 | 177.41 | 209.77 | 383.1 | 177.42 | 192.12 | 900.1 | 86.17 | 226.67 | 2769.3 | 37.43 |
| 218.57 | 744.2 | 85.32 | 210.81 | 1626.8 | 38.17 | 197.48 | 1895.2 | 38.52 | 229.08 | 889.4 | 133.67 |
| 219.52 | 740.0 | 85.43 | 212.17 | 503.6 | 133.71 | 198.56 | 603.8 | 134.22 | 229.22 | 892.6 | 133.67 |
| 219.93 | 485.1 | 134.06 | 212.98 | 774.3 | 85.71 | 200.32 | 919.7 | 86.03 | 230.06 | 2803.2 | 37.34 |
| 221.35 | 743.3 | 85.40 | 213.69 | 386.8 | 177.42 | 200.84 | 926.6 | 85.64 | 231.05 | 1362.1 | 85.36 |
| 221.38 | 489.4 | 134.04 | 214.64 | 777.0 | 85.68 | 201.71 | 1943.3 | 38.40 | 234.17 | 671.0 | 177.44 |
| 221.59 | 1585.3 | 36.86 | 214.92 | 1659.6 | 37.26 | 203.88 | 935.2 | 85.58 | 234.61 | 2843.8 | 37.21 |
| 221.62 | 1034.1 | 61.73 | 215.60 | 388.3 | 177.42 | 206.73 | 1978.6 | 38.27 | 235.27 | 901.6 | 133.61 |
| 223.26 | 488.8 | 134.03 | 216.33 | 388.6 | 177.42 | 208.74 | 619.4 | 134.13 | 235.95 | 697.1 | 177.44 |
| 225.01 | 749.4 | 85.33 | 216.36 | 1614.9 | 38.02 | 209.28 | 949.2 | 85.48 | 236.88 | 675.1 | 177.44 |
| 225.99 | 368.1 | 177.41 | 216.60 | 780.9 | 85.65 | 209.58 | 947.2 | 85.86 | 236.91 | 907.8 | 133.60 |
| 226.73 | 497.2 | 134.16 | 218.35 | 510.1 | 133.66 | 211.27 | 2010.2 | 38.14 | 239.60 | 1390.8 | 85.20 |
| 226.81 | 492.9 | 134.00 | 220.12 | 380.2 | 177.42 | 215.08 | 475.4 | 177.41 | 239.60 | 2890.4 | 37.08 |
| 226.89 | 1610.8 | 36.72 | 220.28 | 1677.1 | 37.11 | 215.70 | 2040.6 | 38.02 | 241.19 | 677.3 | 177.44 |
| 227.71 | 1052.5 | 61.60 | 220.39 | 786.1 | 85.58 | 218.32 | 632.7 | 134.05 | 241.71 | 914.1 | 133.55 |
| 228.04 | 755.3 | 85.27 | 220.69 | 1633.7 | 37.90 | 218.84 | 2106.7 | 37.60 | 245.40 | 2945.2 | 36.92 |
| 228.04 | 759.9 | 85.15 | 220.97 | 1677.9 | 37.09 | 219.06 | 2063.6 | 37.93 | 246.06 | 1413.5 | 85.09 |
| 231.41 | 498.5 | 133.96 | 222.17 | 789.7 | 85.55 | 221.35 | 970.2 | 85.65 | 248.34 | 931.6 | 133.50 |
| 232.97 | 1642.9 | 36.55 | 223.50 | 1649.1 | 37.83 | 222.25 | 485.5 | 177.41 | 248.39 | 680.2 | 177.44 |
| 233.19 | 765.5 | 85.05 | 224.87 | 794.8 | 85.50 | 224.71 | 488.9 | 177.41 | 252.11 | 934.4 | 133.46 |
| 234.09 | 502.2 | 133.93 | 225.01 | 517.9 | 133.60 | 224.98 | 648.5 | 133.99 | 253.08 | 1437.3 | 84.96 |
| 234.50 | 1069.5 | 61.44 | 225.14 | 784.0 | 86.25 | 226.84 | 2115.9 | 37.72 | 255.70 | 682.1 | 177.44 |
| 234.66 | 1675.8 | 36.51 | 228.29 | 384.5 | 177.42 | 227.27 | 2158.3 | 37.37 | 259.97 | 1460.8 | 84.83 |
| 235.68 | 768.1 | 85.14 | 229.71 | 1721.8 | 36.85 | 228.72 | 990.9 | 85.52 | 261.63 | 951.5 | 133.38 |
| 236.78 | 502.7 | 133.91 | 230.48 | 807.2 | 85.40 | 231.02 | 650.9 | 133.94 | 262.07 | 683.1 | 177.43 |
| 237.13 | 376.3 | 177.41 | 231.30 | 525.9 | 133.54 | 231.16 | 2144.2 | 37.60 | 264.37 | 686.2 | 177.43 |
| 237.35 | 770.8 | 85.11 | 231.65 | 1692.6 | 37.60 | 231.68 | 659.1 | 133.93 | 265.39 | 1479.5 | 84.73 |
| | | | | | | | | | 266.30 | 963.9 | 133.34 |

## Literature Cited


(1) Fannin, Jr., A. A., King, L. A., Frank J. Seiler Research Laboratory Technical Report SRL-TR-76-19 (1976).
(2) Fisher, W., Rahlfs, O., *Z. Anorg. Allg. Chem.*, **205**, 1 (1932).
(3) "JANAF Thermochemical Tables", Dow Chemical Co., Midland, Mich., 1974.

(4) King, L. A., Seegmiller, D. W., J. Chem. Eng. Data, 16, 23 (1971).
(5) Sears, J. E., Proc. Phys. Soc., London, 26, 95 (1913); "International Critical Tables", Vol. II, McGraw-Hill, New York, N.Y., 1927, p 457.
(6) Seegmiller, D. W., Fannin, Jr., A. A., Olson, D. S., King, L. A., J. Chem. Eng. Data, 17, 295 (1972).
(7) Smits, A., Meijering, J. L., Z. Phys. Chem., Abt. B, 41, 98 (1938).
(8) Viola, J. T., Seegmiller, D. W., Fannin, Jr., A. A., King, L. A., J. Chem. Eng. Data, 22, 367 (1977).
(9) Vrieland, G. E., Stull, D. R., J. Chem. Eng. Data, 12, 532 (1967).

Received for review May 26, 1977. Accepted November 15, 1977.

# Vapor Pressure of Aluminum Chloride Systems. 3. Vapor Pressure of Aluminum Chloride–Sodium Chloride Melts

**John T. Viola, Lowell A. King,* Armand A. Fannin, Jr., and David W. Seegmiller**

*Frank J. Seiler Research Laboratory (Air Force Systems Command) and Department of Chemistry and Biological Sciences, United States Air Force Academy, Colorado 80840*

**The vapor pressures of liquid aluminum chloride–sodium chloride mixtures containing 53–74 mol % aluminum chloride were measured from the condensation temperatures of solid aluminum chloride to 251 °C. Samples were contained in Pyrex isoteniscopes which utilized mercury as the manometric fluid. The mercury columns were brought to null by an external pressure which was in turn measured at each experimental point. The experimental pressures were fit to a single equation which serves the entire composition–temperature region.**

We measured the vapor pressure of aluminum chloride–sodium chloride molten mixtures as part of our continuing investigation of low-melting molten salt battery electrolytes. Previously reported vapor pressures of this system (*2*, *3*, *5*, *6*) are in disagreement by more than an order of magnitude.

## Experimental Section

Preparation of the $AlCl_3$, the glovebox atmosphere, loading of the isoteniscope, the constant temperature bath and its temperature regulation and measurement, and the measurement of vapor pressure were all as described previously (*10*). A mercury manometer was used as an additional external pressure measurement device.

Powdered mixtures of $AlCl_3$ and NaCl were loaded into a Pyrex isoteniscope similar to that used for saturated $AlCl_3$ vapor pressures (*10*). NaCl was dried by maintaining it molten for several hours (*7*). The $AlCl_3$–NaCl mixtures were prepared by grinding and mixing weighed amounts of $AlCl_3$ crystals with weighed amounts of dry NaCl crystals in a glovebox.

## Results

A total of 227 measurements on 12 different compositions were taken at values of mole fraction and temperature that lay within a polygon on the $X,t$ plane described approximately by the coordinates ($X$, $t$) = (0.54, 149), (0.58, 106), (0.61, 103), (0.70, 175), (0.74, 182), (0.74, 251), and (0.54, 251). Pressure measurements were made at both ascending and descending temperature steps, and equilibrium was assured at each point by maintaining constant temperature for many minutes until pressure remained constant within measurement error. The samples were stirred by vigorous shaking before each measurement to prevent the formation of internal concentration gradients.

The data are given in Table I. Pressures have been corrected for the vapor pressure of mercury within the isoteniscope. Interactions between $Al_2Cl_6$ vapor and Hg vapor were assumed to be negligible. The measurement method for each datum is indicated in the table. Several additional measurements were made at temperatures lying below the $X,t$ polygon for each of the eight compositions richest in $AlCl_3$. These pressures lay on the curve of saturated vapor pressure of solid $AlCl_3$ (*10*), and fell distinctly away from the $X,p,T$ surface for $AlCl_3$–NaCl melts.

We assumed the vapor pressure of $AlCl_3$–NaCl melts could be represented by an equation of the form

$$\log p = (A/T) + B \tag{1}$$

where

$$A = A_0 + A_1X + A_2X^2$$
$$B = B_0 + B_1X + B_2X^2 \tag{2}$$

The vapor pressures of individual compositions were fit by other investigators to equations of the form of eq 1 (*3*, *5*, *6*) or eq 1 modified by the addition to the right-hand side of the term $\Delta C_p/R \log T$ (*1*, *2*).

The data were least-squares fit in such a way as to minimize the perpendicular distance, $z$, from the experimental points to the function surface in $X$, $p$, and $T$ given by eq 1 and 2. This procedure is similar to the fitting technique used earlier (*10*). The equations were solved for the values of $A_j$ and $B_j$ which minimized the sum, $\sum_{i=1}^{N} z_i^2$ where

$$z_i = \left[\left(\frac{\delta p_i}{\Delta p_i}\right)^2 + \left(\frac{\delta T}{\Delta T_i}\right)^2\right]^{-1/2} \tag{3}$$

In eq 3, $\delta p_i$ = the greater of 0.1 Torr or 0.005 $p$, $\delta T$ = 1 K, $\Delta p_i = p_{exp,i} - \exp[(A_i/T_{exp,i} + B_i) \ln (10)]$, and $\Delta T_i = T_{exp,i} - A_i/(\log p_{exp,i} - B_i)$. As indicated in eq 2, $A$ and $B$ are functions of $X$. Since there was an appreciable vapor space in the isoteniscope (ca. 85 $cm^3$), the true mole fraction, $x$, of the melt will be different for each experimental point, depending upon the nominal mole fraction, $X$, and upon temperature. Accordingly, for every experimental point

$$A_i = A_0 + A_1x_i + A_2x_i^2$$
$$B_i = B_0 + B_1x_i + B_2x_i^2 \tag{4}$$